Revealing the Source of the Radial Flow Patterns in Proton-Proton Collisions using Hard Probes

Antonio ~~Ortíz~~Ortiz[1], Gyula Bencédi[1,3], Héctor Bello[1,2]

[1] Instituto de Ciencias Nucleares, UNAM, México City
[2] Facultad de Ciencias Físico Matemáticas, BUAP, 1152, Puebla, México
[3] Wigner Research Centre for Physics of the HAS, Budapest, Hungary

E-mail: Gyula.Bencedi@cern.ch

Abstract.

In this work, we propose a tool to reveal the origin of the collective-like phenomena observed in proton-proton collisions. We exploit the fundamental difference between the underlying mechanisms, color reconnection (CR) and hydrodynamics, which produce radial flow patterns in Pythia 8 and Epos 3, respectively. ~~Namely~~Specifically, the strength of the coupling between the soft and hard components which by construction is larger in Pythia 8 than in Epos 3.

For simulations of minimum bias pp collisions at $\sqrt{s} = 7\,\text{TeV}$, we study the transverse momentum (p_{T}) distributions of charged pions, kaons and (anti)protons as a function of the event multiplicity and the transverse momentum of the leading jet ($p_{\text{T}}^{\text{jet}}$), being all of them determined within a pseudorapidity interval of $|\eta| < 1$. Quantitative and qualitative differences between Pythia 8 and Epos 3 are found in the p_{T} spectra when (for a given multiplicity class) the leading jet p_{T} is increased. In addition, we show that for low-multiplicity events jets can produce radial flow-like behaviour. We propose to perform a similar analysis using data from RHIC and LHC.

Keywords: Color reconnection, hydrodynamics, particle production, ~~particle ratios,~~ proton-proton collision, radial flow

Submitted to: *J. Phys. G: Nucl. Part. Phys.*

1. Introduction

The study of particle production in high-multiplicity events in small collision systems at the LHC has revealed unexpected new collective-like phenomena. In particular, for high-multiplicity proton-proton (pp) and proton-lead (~~ppb~~p-Pb) collisions, radial flow signals [1, 2], long-range angular correlations [3, 4], and the strangeness enhancement [5, 6, 7] have been reported. Those effects are well known in heavy-ion collisions, where they are attributed to the existence of the strongly interacting Quark-Gluon Plasma (QGP) [8, 9, 10]. Understanding the phenomena is crucial because for heavy-ion physics, pp and ~~ppb~~ p-Pb collisions have been used as the baseline ("vacuum") to extract the genuine QGP effects. However, it is worth mentioning that no jet quenching effects have been found so far in ~~ppb~~ p-Pb collisions [11], suggesting that other mechanisms could also play a role in producing collective-like behaviour in small collision systems [12, 13].

Hydrodynamic calculations reproduce many of the observations qualitatively [14]. However, it has also been found that multi-parton interactions (MPI) [15] and color reconnection (CR) as implemented in Pythia [16] produce radial flow patterns via boosted color strings [17]. Moreover, within the dilute-dense limit of the color glass condensate, it has been demonstrated that the physics of fluctuating color fields can generate azimuthal multi-particle correlations [18]; and the mass ordering of elliptic flow when the fragmentation implemented in Pythia is included [19]. The same observable has been studied using the multi-phase transport model [20], where the ridge structure can be generated assuming incoherent elastic scatterings of partons and the string melting mechanism. Other mechanisms like "color ropes", which are formed by the fusion of color strings close in space, can increase both the strangeness production and the radial flow-like effects [21].

The measurements of the transverse momentum (p_{T}) spectra of identified particles as a function of event multiplicity in pp collisions at the LHC [5, 22] have shown that models fail to describe the data quantitatively. Therefore, the results of those comparisons alone are not enough to give desired information about the origin of the observed effects (i.e. radial flow-like patterns). In order to extract more information, we propose the implementation of a differential study based on the classification of the events according to event multiplicity and the jet content.

In ~~heavy-ion collisions by studying this soft region one can naturally quantify the effect of radial flow. In the~~ the so-called MPI-based model of color reconnection [16], the interaction between scattered partons at soft and at hard p_{T} scales is imposed ~~. The event-by-event partonic scatterings are mostly associated with~~ as follows. All gluons of low-p_{T} interactions ~~, albeit the~~ can be inserted onto the colour-flow dipoles of a higher-p_{T} one, keeping the total string length as short as possible. Since the probability of having a hard scattering increases with the number of MPI~~. An interplay between soft and hard scatterings mediated by color strings is therefore expected to provide~~ , color reconnection can give a strong correlation between the radial flow-like patterns and the hard component of the collision [23] in high multiplicity events.

On the contrary, in the scenario where the hydrodynamical evolution of the system is the prime mechanism, jets are not expected to strongly modify the radial flow patterns. Albeit hard partons cannot thermalize, momentum loss of jets could affect the fluid dynamic evolution of the medium. However, the effect has been studied for heavy-ion collisions and it was found to give only a minor correction [?]. In the present paper we argue that by exploiting such a fundamental difference between both models, one might say whether or not the observed effects are driven by hydrodynamics. To this end, we propose a systematic study by analysing the mid-rapidity ($|y| < 1$) inclusive p_{T} spectra of identified charged hadrons as a function of the mid-pseudo-rapidity ($|\eta| < 1$) event multiplicity (N_{ch}) and transverse momentum of the leading jet ($p_{\mathrm{T}}^{\mathrm{jet}}$). This study was carried out using Pythia 8.212 and Epos 3.117 Monte Carlo (MC) event generators, from now on referred to as Pythia 8 and Epos 3, respectively.

The paper is organised as follows: In section 2, some important features of the Monte Carlo event generators and the jet finder are outlined, with special emphasis on those aspects which are relevant in this study. In section 3, the results and discussion are presented. Finally in section 4, the conclusions and the outlook are given.

2. Simulation setup and Monte Carlo models

The studies were carried out for pp collisions at the centre-of-mass energy of $\sqrt{s} = 7\,\mathrm{TeV}$ considering sets with and without the mechanism which produces radial flow patterns.

The results are presented both for Pythia 8 and Epos 3 using primary charged particles, defined as all charged particles produced in the collision including the products of strong and electromagnetic decays but excluding products of weak decays. Unless stated otherwise, no requirement on the minimum p_{T} of the particles is applied in any of the results. All MC generators use parton-to-hadron fragmentation approaches fitted to the experimental data – such as the Lund string [24] and area law hadronization [25] models.

For the results presented in this paper we generated ~~$\approx 10^2$ million events for the so-called~~ $\approx 10^2$ million "minimum bias" (MB) ~~interactions,~~ events, including diffractive and non-diffractive events, which were subsequently split into sub-samples based on the selection of charged particle multiplicity and hardness of the event. The MB term refers commonly to inelastic interactions experimentally measured using a generic minimum-bias trigger that accepts a large fraction of the particle production cross section by requiring a minimum activity in one or more detectors.

2.1. Epos *3 and hydrodynamics*

Epos 3 [26, 27] is a generator of complete events (soft + hard components) which contains hard scatterings and MPI. For high string densities, e.g. achieved in high-

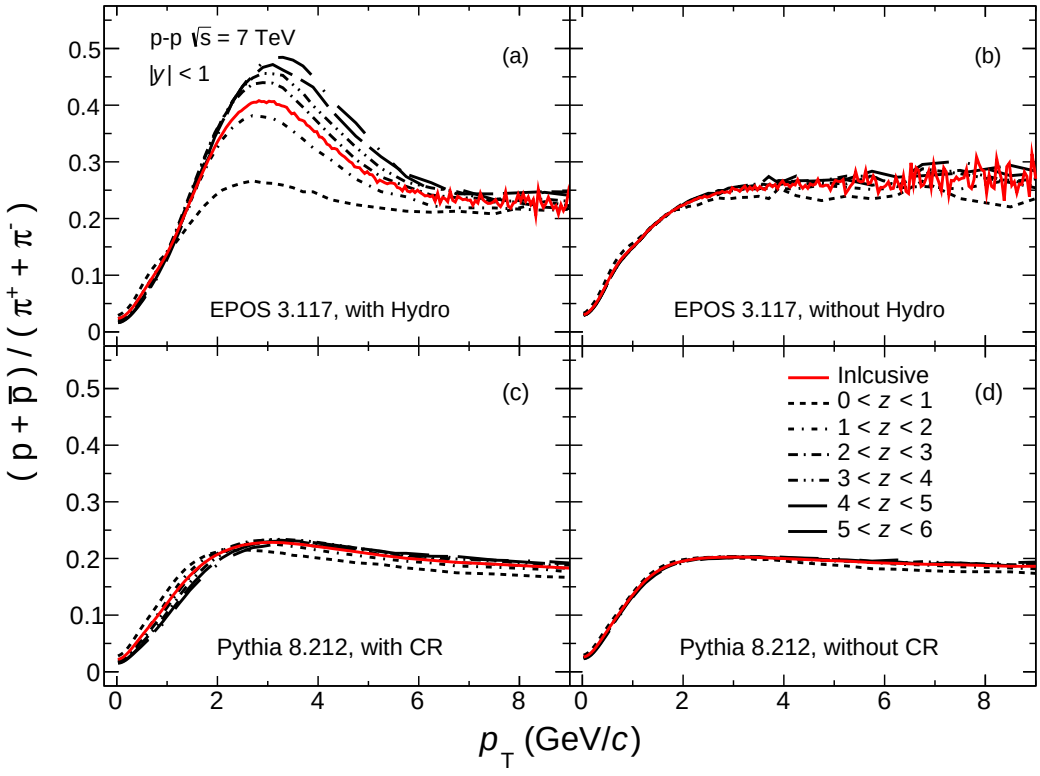

Figure 1: (Color online) Proton-to-pion ratio as a function of p_{T} for different multiplicity event classes. Results for pp collisions at $\sqrt{s} = 7\,\mathrm{TeV}$ generated with EPOS 3 and PYTHIA 8 are presented. For PYTHIA 8 (EPOS 3) the ratios are displayed for simulations with and without color reconnection (hydrodynamical evolution of the system).

multiplicity pp collisions, the model does not allow the strings to decay independently, instead, if energy density from string segments is high enough they fuse into the so-called "core" region, which evolves hydrodynamically. On the other hand, the low energy density region forms the "corona" which hadronizes using the unmodified string fragmentation.

The "core" region originates around 30% of the central particle production for an average pp collision at $\sqrt{s} = 7\,\mathrm{TeV}$, $\langle \mathrm{d}N_{\mathrm{ch}}/\mathrm{d}\eta \rangle_{|\eta|<2.4} \approx 6.25$. This fraction might reach $\approx 75\%$ for $\langle \mathrm{d}N_{\mathrm{ch}}/\mathrm{d}\eta \rangle_{|\eta|<2.4} \approx 20.8$ [28]. Concerning the hard component, the inclusive jet cross section for pp collisions at $\sqrt{s} = 0.2\,\mathrm{TeV}$ obtained with EPOS 3 agrees within 5% and 4% with STAR data and NLO pQCD calculations, respectively [29]. Therefore, an analysis in EPOS 3 as a function of event multiplicity and leading jet transverse momentum makes sense.

To illustrate the effect of hydrodynamics on flow observables, Fig. ~~??~~ 1 shows the proton-to-pion ratio as a function of p_{T} for different multiplicity classes. Results are presented in intervals of z, defined as

$$z = \frac{\mathrm{d}N_{\mathrm{ch}}/\mathrm{d}\eta}{\langle \mathrm{d}N_{\mathrm{ch}}/\mathrm{d}\eta \rangle} \,, \tag{1}$$

where ~~$\langle dN_{ch}/d\eta \rangle$~~ $\langle dN_{ch}/d\eta \rangle (= 5.505)$ is the average mid-rapidity particle density for minimum bias pp collisions at $\sqrt{s} = 7\,\text{TeV}$. It is important to say, that according with ALICE results [5], $\langle dN_{ch}/d\eta \rangle \sim 25$ is large enough to see new phenomena in small systems like the strangeness enhancement. For the simulations presented in this paper, such high multiplicity densities are achieved for $z > 4$. Fig. ~~??~~ 1a shows the case when hydrodynamics is considered in the simulations. In this case, a clear evolution of the particle ratio with z can be observed, e.g. going from the lowest z to the highest z values the particle ratios exhibit a depletion (enhancement) for the transverse momentum interval $p_{\text{T}} < 1\,\text{GeV}/c$ ($1 < p_{\text{T}} < 6\,\text{GeV}/c$). This feature is usually attributed to radial flow which modifies the spectral shapes of the p_{T} distribution depending on the hadron mass. On the contrary, Fig. ~~??~~ 1b shows the case without hydrodynamics, where the particle ratios do not evolve with multiplicity. It is worth noticing that a similar effect is observed in ~~Pythia~~PYTHIA 8 (Figures 1c and 1d), but in that case the radial flow-like behavior is attributed to color reconnection [17].

2.2. PYTHIA *8 and color reconnection*

PYTHIA 8 [16] is a full event generator for pp collisions. For inelastic collisions, which is the main interest here, each collision is modelled via one or more parton-parton interactions. The full calculation involves leading-order (LO) pQCD $2 \to 2$ matrix elements, complemented with initial- and final-state parton radiation, multiple particle interactions, beam remnants and the Lund string fragmentation model. PYTHIA 8 also has strong final-state parton interactions (implemented through the CR models [16]). In this work we use the Monash 2013 tune [30] which has as default parametrisation the so-called MPI-based model of color reconnection. Such a model allows partons of each MPI system to form their own structure in color space and then, they are merged into the color structure of a higher p_{T} MPI system, with a probability $\mathcal{P}$ given by:

$$\mathcal{P}(p_{\text{T}}) = \frac{(R \times p_{\text{T0}})^2}{(R \times p_{\text{T0}})^2 + p_{\text{T}}^2} \,, \tag{2}$$

were R is the reconnection range ($0 \leq R \leq 10$) and p_{T0} is the energy dependent parameter used to damp the low-p_{T} divergence of the $2 \to 2$ QCD cross section.

To illustrate how the Monash 2013 tune describes the data, Fig. 2a shows the proton-to-pion and the kaon-to-pion ratios for inelastic pp collisions at $\sqrt{s} = 7\,\text{TeV}$. As discussed in [17], the model shows a qualitative agreement with data, e.g., the bump in the proton-to-pion ratio, though the size of the effect is underestimated. The same level of accuracy is achieved by EPOS 3 which according to Fig. 2b overestimates the effect when hydrodynamics is included. So, in the end we will compare models which still do not fully describe the data, but this does not matter for our purposes. Because, we want to study differences attributed to the fundamental underlying physics mechanisms which produce the observed radial flow effects.

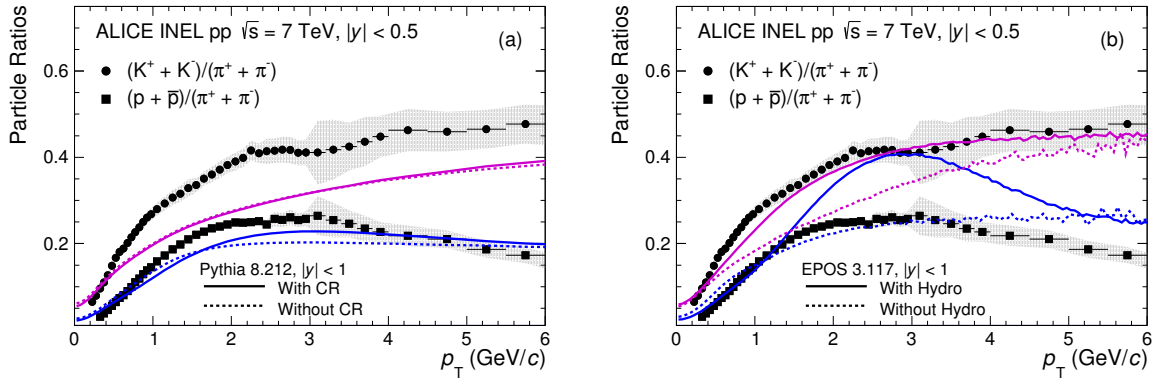

(a) (b)

Figure 2: (Color online) Proton-to-pion ratio as a function of p_{T} for inelastic pp collisions at $\sqrt{s} = 7\,\mathrm{TeV}$ measured by the ALICE Collaboration [2]. Results are compared to models carried out (a) with Pythia 8 and (b) Epos 3 event generators. Cases with and without the effect of color reconnection and hydrodynamics are plotted as solid and dashed lines, respectively

2.3. FastJet *3.1.3 and hardness of the event*

Jets are reconstructed with the anti-k_{T} algorithm implemented in FastJet 3.1.3 [31], using charged and neutral particles, considering a cone radius of 0.4 and a minimum transverse momentum $p_{\mathrm{T,min}}^{\mathrm{jet}} = 5\,\mathrm{GeV}/c$. The lower requirement on the jet p_{T} acts to suppress soft interactions by ensuring that at least one semi-hard scattering is present within the acceptance.

In the following, the jet searching is done within a given pseudorapidity interval, which defines the maximum pseudorapidity of the jet. We tested the performance of FastJet in high ~~multiplicity events. For testing purposes only, we generated pp collisions at $\sqrt{s} = 7\,\mathrm{TeV}$ using the Monash 2013 tune ensuring the production of leading jets with p_{T} of $25\,\mathrm{GeV}/c$ by fixing the minimum and maximum invariant p_{T} ($\hat{p}_{\mathrm{T}}$ for $2\to2$ processes) to 25 and $26\,\mathrm{GeV}/c$, respectively. The jet finder was then run over such a sample considering two pseudorapidity intervals for the jet reconstruction, $|\eta| < 2.4$ and $|\eta| < 1$. Figure **??** shows the p_{T} spectra of the leading jet, within the acceptance, as a function of the event multiplicity~~ pp multiplicity events. ~~When considering the case $|\eta| < 2.4$ in Fig. **??**, a clear peak is observed in the expected $p_{\mathrm{T}}^{\mathrm{jet}}$ region, although a small signal of jets with $p_{\mathrm{T}}^{\mathrm{jet}} = 5\,\mathrm{GeV}/c$ appears in low-multiplicity events. In general, the $p_{\mathrm{T}}^{\mathrm{jet}}$ spectra are not narrow because initial- and final-state radiation may change the transverse momentum of the reconstructed jet. In addition, the probability of finding the leading jet of the event is expected to be reduced if the pseudorapidity interval for the jet searching is restricted, e.g. by using $|\eta| < 1$ instead of $|\eta| < 2.4$. This explains the results for $|\eta| < 1$, shown in Fig. **??**, where a peak at $p_{\mathrm{T}} \approx 24\,\mathrm{GeV}/c$ is present together with a large contribution from jets with $p_{\mathrm{T}}^{\mathrm{jet}} < 24\,\mathrm{GeV}/c$. Similar results are obtained when the jet pseudorapidity is restricted to ±0.4. For the studies presented here we use the acceptance of the ALICE's central barrel ($|\eta| < 1$) , albeit the reconstructed jet~~

$\left\langle \frac{dN_{ch}}{d\eta} \right\rangle_{\lvert\eta\rvert<1}$	$\langle p_T^{jet} \rangle_{\lvert\eta\rvert<1}$ (GeV/c)	% of events with $p_T^{jet} > 5$ GeV/c
2.12 ($0 < z < 1$)	7.09	1.03
8.12 ($1 < z < 2$)	7.49	13.1
13.6 ($2 < z < 3$)	7.83	37.3
19.0 ($3 < z < 4$)	8.48	63.7
24.4 ($4 < z < 5$)	9.56	83.2
29.8 ($5 < z < 6$)	11.1	93.9
35.2 ($6 < z < 7$)	13.2	98.2
40.6 ($7 < z < 8$)	16.1	99.5
46.1 ($8 < z < 9$)	19.7	99.8

Table 1: Charged-particle pseudorapidity densities at central pseudorapidity ($|\eta| < 1$), for pp collisions at $\sqrt{s} = 7$ TeV simulated with PYTHIA 8 having jets with p_T above 5 GeV/c in the same region. The multiplicity classes are presented along the leading jet p_T and the fraction of events where a jet with p_T above 5 GeV/c was identified.

~~could not be the leading one.~~

~~These results suggest that the jet finder is suitable for the proposed analysis as a function of the event multiplicity in minimum bias pp collisions‡ as presented in the next section~~

It is also important to mention that the FastJet package has been successfully used in more challenging environments (central heavy-ion collisions) than those reported in this paper.

3. Results and discussion

3.1. Multiplicity dependence of the leading jet p_T

By running FASTJET (considering cone radius 0.4, $|\eta| < 1$ and $p_{T,min}^{jet} = 5$ GeV/c) over the MB sample generated with PYTHIA 8 we obtain the results for the average mid-pseudo-rapidity densities, presented in Table 1.
Going from $\langle dN_{ch}/d\eta \rangle = 19$ to $\langle dN_{ch}/d\eta \rangle = 46.1$, the average leading jet p_T ranges from 8.48 GeV/c up to 19.7 GeV/c. A similar behavior was found for the leading parton transverse momentum, obtained at mid-pseudorapidity, as a function of $\langle dN_{ch}/d\eta \rangle$. The effect is explained in the context of multi-partonic interactions, because the probability of finding a hard parton is expected to be larger in high-multiplicity events (large average N_{mpi}) than in low-multiplicity events (small average N_{mpi}). This effect is also reflected in the behaviour of the fraction of events having at least one jet with momentum above

‡ ~~Moreover, this jet finder has been successfully applied in much challenging environments like central heavy-ion collisions at the LHC [32].~~

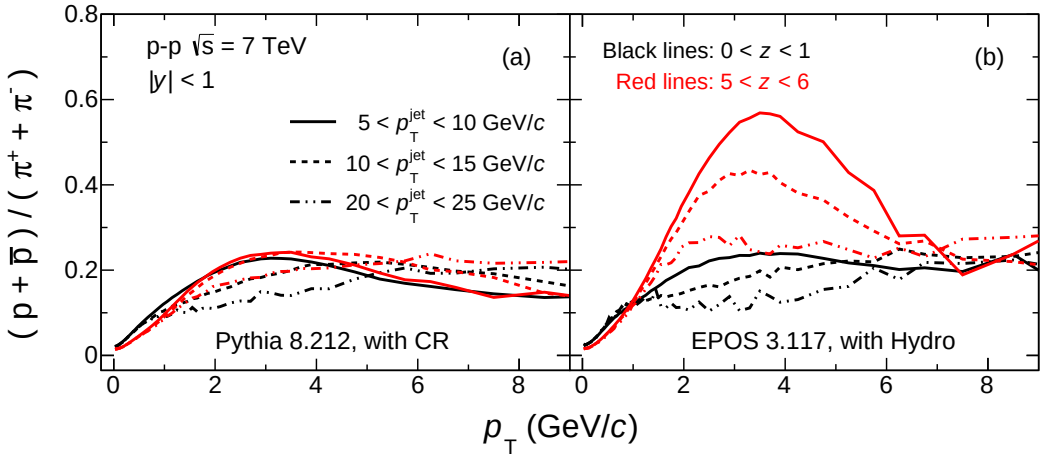

Figure 3: (Color online) Inclusive proton-to-pion ratio as a function of $p_{\rm T}$ for two multiplicity classes, $0 < z < 1$ (black lines) and $5 < z < 6$ (red lines); and for different $p_{\rm T}^{\rm jet}$ intervals. Results are shown for both (a) PYTHIA 8 and (b) EPOS 3.

5 GeV/c.

3.2. Proton-to-pion ratio as a function of $N_{\rm ch}$ and $p_{\rm T}^{\rm jet}$

Figure 3 shows the inclusive proton-to-pion ratio as a function of $p_{\rm T}$ for events with low and high z. Regarding the low-z case ($0 < z < 1$), the results indicate that for $5 < p_{\rm T}^{\rm jet} < 10\,{\rm GeV}/c$ the ratios exhibit a bump at $p_{\rm T} \approx 3\,{\rm GeV}/c$ for both EPOS 3 and PYTHIA 8. Whereas, for higher $p_{\rm T}^{\rm jet}$ the position of the peak is shifted to higher $p_{\rm T}$. This observation suggests that the bump is not an exclusive effect of radial flow (as suggested by Fig. ??1), but also a feature of the fragmentation. It is worth noticing that the same effect has been observed in ALICE data, where the jet hadrochemistry has been measured in minimum bias pp collisions at $\sqrt{s} = 7\,{\rm TeV}$ [33].

Also shown in Fig. 3 the multiplicity class $5 < z < 6$, where we see that the maximum of the proton-to-pion ratio increases with increasing multiplicity, being much larger for EPOS 3 than for PYTHIA 8. The EPOS 3 event class $5 < p_{\rm T}^{\rm jet} < 10\,{\rm GeV}/c$ exhibits an enhancement of $({\rm p}+\bar{\rm p})/(\pi^+ + \pi^-)$ with respect to the inclusive case (Fig. ??1 without any selection on $p_{\rm T}^{\rm jet}$). While for higher $p_{\rm T}^{\rm jet}$ the position of the peak is shifted to lower $p_{\rm T}$ values and the size of the peak is significantly smaller than that for the inclusive case. The effect is quantitatively and qualitatively different in PYTHIA 8, namely, the size of the peak does not change with increasing $p_{\rm T}^{\rm jet}$, instead it is just shifted to higher $p_{\rm T}$. In EPOS 3 the effect vanishes when hydrodynamics is switched off, and therefore it can be a consequence of the "core-corona" separation, where low-momentum partons are more likely forming the "core" region. It is worth mentioning that this difference between the two event classes could contribute to the differences observed in the hadrochemistry measured in the so-called "bulk" (outside the jet peak) and the jet regions in p-Pb and Pb-Pb collisions at the LHC [34, 35]. In summary, an

analysis of data as a function of multiplicity and hardness provides a more powerful tool for testing the aforementioned models than that which only uses multiplicity.

3.3. Blast-wave model fits

Color reconnection, without any hydrodynamical component, produces radial flow-like patterns in events simulated with PYTHIA 8 [17]. Such a conclusion was based on the good agreement between the Boltzman-Gibbs blast-wave model and the p_{T} spectra of different particle species. The blast-wave model describes a locally thermalised medium which experiences a collective expansion with a common velocity field and undergoing an instantaneous common freeze-out [36]. From the simultaneous fit of the blast-wave model to the p_{T} spectra of different particle species we extract two parameters, which in the hot and dense QCD systems created in heavy-ion collisions, are related to the temperature at the kinetic freeze-out, T_{kin}, and the average transverse expansion velocity, $\langle\beta_{\mathrm{T}}\rangle$. In the current study we considered p_{T} ranges: ~~$0.5 < p_{\mathrm{T}}^{\mathrm{jet}} < 1.0$~~$0.5 < p_{\mathrm{T}} < 1.0\,\mathrm{GeV}/c$, ~~$0.3 < p_{\mathrm{T}}^{\mathrm{jet}} < 1.5$~~$0.3 < p_{\mathrm{T}} < 1.5\,\mathrm{GeV}/c$ and ~~$0.8 < p_{\mathrm{T}}^{\mathrm{jet}} < 2.0$~~$0.8 < p_{\mathrm{T}} < 2.0\,\mathrm{GeV}/c$ to fit the model to the p_{T} distributions of charged pions, kaons and (anti)protons, respectively. The specific selection of the p_{T} ranges mentioned above was successfully applied in our previous studies [37] where the parametrizations, obtained from the fits, described within 10% the strange and multi-strange p_{T} spectra.

For pp collisions at $\sqrt{s} = 7\,\mathrm{TeV}$ simulated with PYTHIA 8, Fig. 4 shows the p_{T} spectra of charged pions, kaons and (anti)protons for two multiplicity classes, $0 < z < 1$ and $5 < z < 6$, ~~and~~ being each one split in three specific ~~leading jet~~ subclasses. The first subclass, treated as a baseline since no jets at mid-pseudorapidity are found, is compared with samples where low (5-10 GeV/c) and high (20-25 GeV/c) p_{T} ~~intervals~~jets are produced. There are some interesting observations one might read off from this analysis:

- Even at extremely low multiplicity ($0 < z < 1$), where color reconnection effects are negligible, it is possible to find an event class where the radial flow-like patters pop up. Especially, in events having $p_{\mathrm{T}}^{\mathrm{jet}} > 5\,\mathrm{GeV}/c$ the p_{T} distributions of identified hadrons are better described by the blast-wave model than in those without jets. It is worth mentioning that recently the CMS collaboration has reported that in low-multiplicity pp events, the elliptic flow Fourier harmonic is not zero [4], supporting the idea that other mechanisms could produce the collective-like behaviour.
- At high multiplicity, the blast-wave model fails to describe the p_{T} spectra when CR is not included in the simulations, this behaviour is also observed even if a jet with $p_{\mathrm{T}}^{\mathrm{jet}} > 5\,\mathrm{GeV}/c$ is produced at mid-rapidity. On the other hand, with CR the agreement between the blast-wave parametrization and the p_{T} spectra improves with increasing $p_{\mathrm{T}}^{\mathrm{jet}}$. This just reflects that in PYTHIA 8 the interaction between jets and the underlying event is crucial for generating a collective-like behaviour.

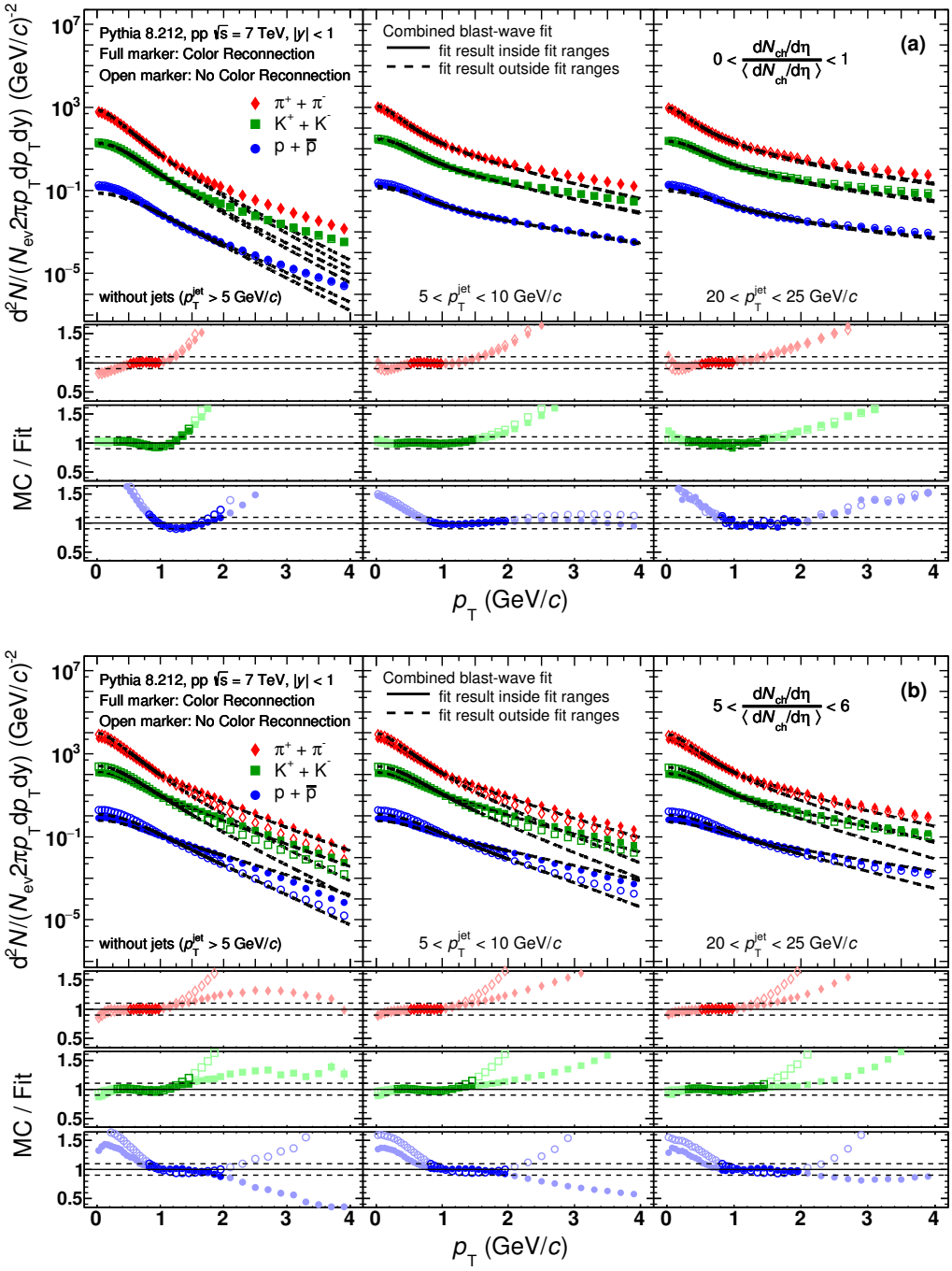

Figure 4: (Color online) Transverse momentum distributions of charged pions, kaons and (anti)protons for (a) low- and (b) high-multiplicity pp collisions at $\sqrt{s} = 7\,\text{TeV}$ generated with PYTHIA 8. For each multiplicity class, three sub-samples are shown, from left to right, events without a leading jet with $p_{\text{T}}^{\text{jet}} > 5\,\text{GeV}/c$, with $5 < p_{\text{T}}^{\text{jet}} < 10\,\text{GeV}/c$ and with $20 < p_{\text{T}}^{\text{jet}} < 25\,\text{GeV}/c$, respectively. Results for the cases with and without color reconnection are plotted with full and empty markers, respectively. The parametrizations obtained from the simultaneous blast-wave fits are shown as solid lines. The ratio of the p_{T} spectrum to the blast-wave model fit is shown in the bottom plots, indicating the fitting range using dark colors

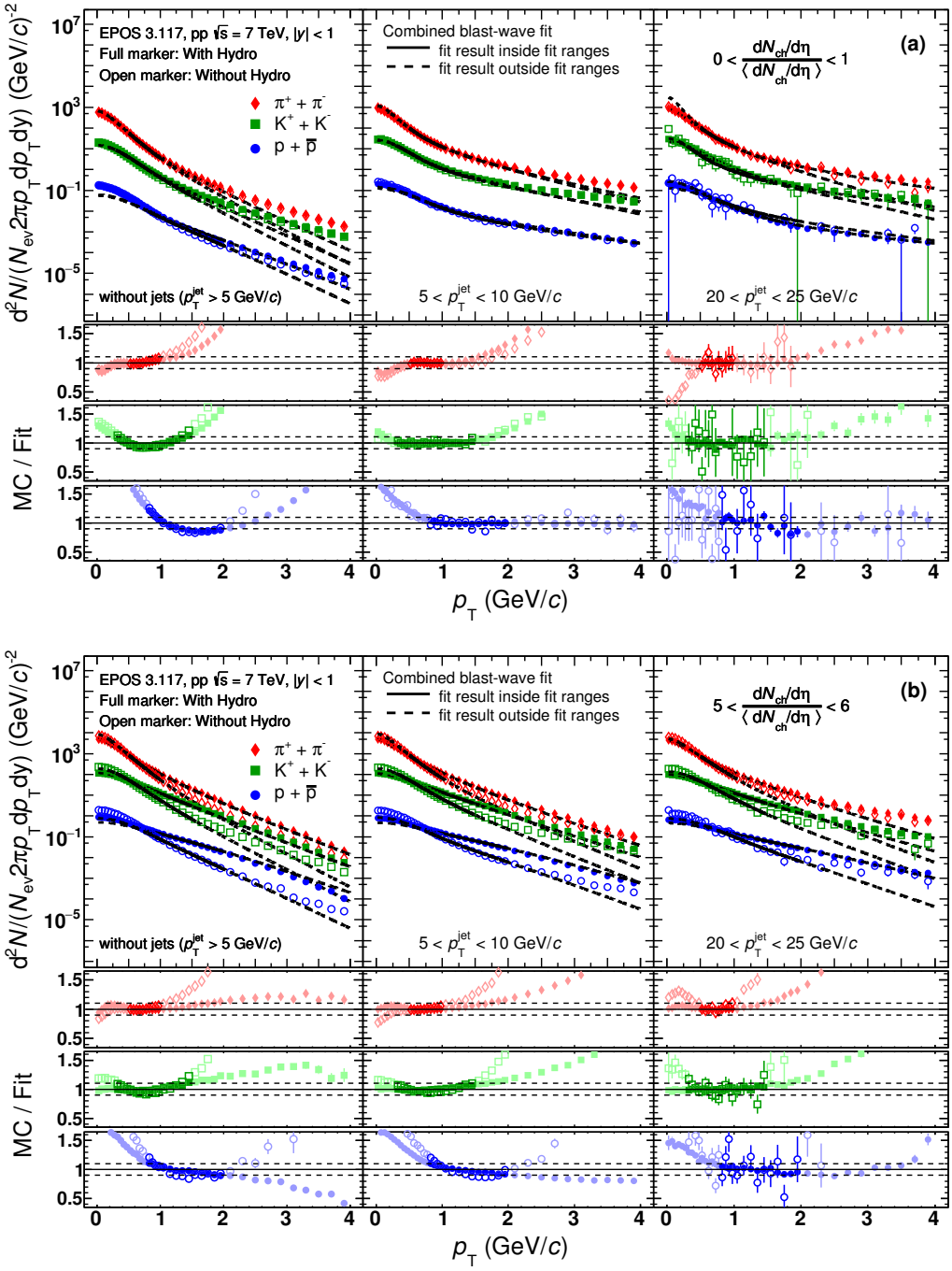

Figure 5: (Color online) Transverse momentum distributions of charged pions, kaons and (anti)protons for (a) low- and (b) high-multiplicity pp collisions at $\sqrt{s} = 7\,\text{TeV}$ generated with Epos 3. For each multiplicity class, three sub-samples are shown. From left to right, events without a leading jet with $p_{\text{T}}^{\text{jet}} > 5\,\text{GeV}/c$, with $5 < p_{\text{T}}^{\text{jet}} < 10\,\text{GeV}/c$ and with $20 < p_{\text{T}}^{\text{jet}} < 25\,\text{GeV}/c$, respectively. Results for the cases with and without hydrodynamics are plotted with full and empty markers, respectively. The parametrizations obtained from the simultaneous blast-wave fits are shown as solid lines. The ratio of the p_{T} spectrum to the blast-wave model fit is shown in the bottom plots, indicating the fitting range using dark colors

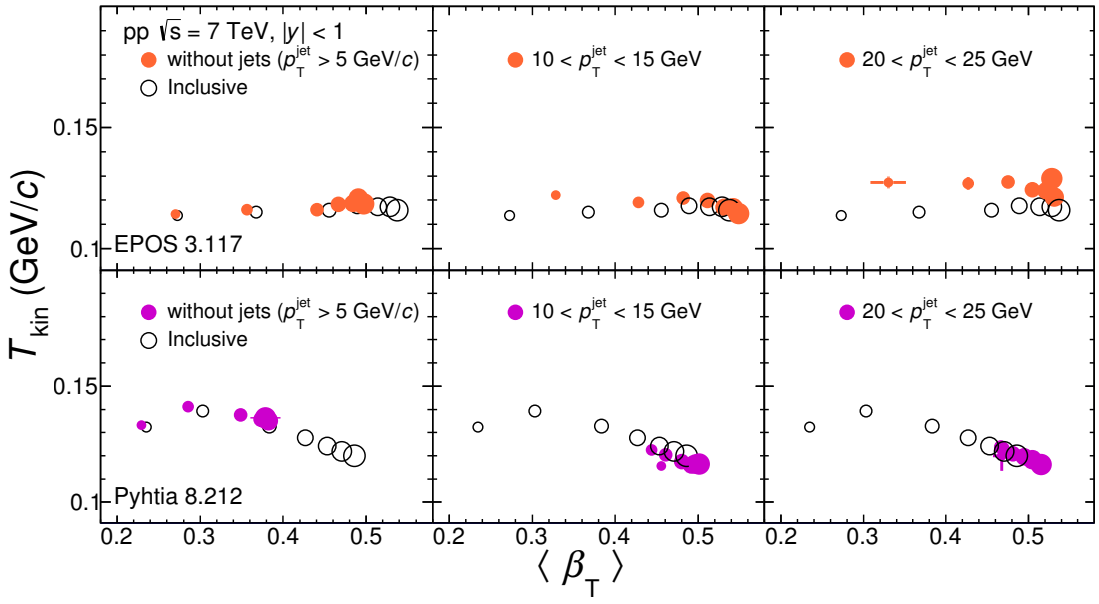

Figure 6: (Color online) Correlation between two parameters obtained from the blast-wave analysis, the temperature ($T_{\rm kin}$) and the average transverse expansion velocity ($\langle\beta_{\rm T}\rangle$) of the system. Results for pp collisions at $\sqrt{s} = 7\,\text{TeV}$ simulated with Epos 3 and Pythia 8 are presented in the top and the bottom panels, respectively. The size of the markers increases with the event multiplicity. Results with (full markers) and without (empty markers) a selection on $p_{\rm T}^{\rm jet}$ are compared

In Fig. 5 analogous effects are shown for Epos 3 simulations, though the jet contribution to the radial flow patterns is smaller than in Pythia 8. To quantify the importance of jets in events where flow patterns are generated with hydrodynamics or color reconnection, Fig. 6 shows the correlation between the blast-wave parameters $T_{\rm kin}$ and $\langle\beta_{\rm T}\rangle$. Results are shown for different z multiplicity classes, which are indicated by different marker sizes and increase from low $\langle\beta_{\rm T}\rangle$ to high $\langle\beta_{\rm T}\rangle$. Beside the multiplicity selection, also shown the case when we consider the selection on the hardness of the event.

- For events having jets and being in the same multiplicity class (same marker size), $\langle\beta_{\rm T}\rangle$ increases with respect to the case without any selection on the hardness (inclusive case). By looking at, for example, the case of jets with $20 < p_{\rm T}^{\rm jet} < 25\,\text{GeV}/c$ and the highest multiplicity class ($5 < z < 6$), the effect is weaker in Epos 3 ($\approx 0.6\%$) than in Pythia 8 ($\approx 6.8\%$). This is also illustrated in the larger multiplicity dependence of $\langle\beta_{\rm T}\rangle$ obtained in Epos 3 than in Pythia 8.
- On the other hand, for events without jets, the multiplicity dependence of $\langle\beta_{\rm T}\rangle$ is weaker in Epos 3 than in Pythia 8. In Pythia 8 the $\langle\beta_{\rm T}\rangle$ reach is much smaller than in Epos 3.

4. Conclusions

In this work, we have presented a study using two event generators, EPOS 3 and PYTHIA 8, exploring an observable which is aimed for ruling out or validating the underlying physics mechanism (hydrodynamics or color reconnection) generating radial flow patterns in pp collisions. Specifically, we exploit the fact that, by construction, color reconnection produces a strong coupling between the hard (hard partons) and soft (soft and semi-hard partons) components of the interaction. To this end, we have studied the p_{T} spectra of charged pions, kaons and (anti)protons as a function of the event multiplicity and the transverse momentum of the leading jet. The main findings are listed below.

- In extremely low multiplicity events ($0 < z < 1$), where hydrodynamics definitely cannot be applied and where color reconnection effects are small, we observe a flow-like peak in the proton-to-pion ratio. Furthermore, the blast-wave parametrizations simultaneously describe the p_{T} spectra for the different particle species, the agreement between the model and the p_{T} spectra significantly improves with increasing the leading jet p_{T}. Hence, we observe collective-like behavior even in low-multiplicity events but caused by jets.
- For high-multiplicity events, the particle composition is very different in PYTHIA 8 and EPOS 3. In EPOS 3 the size of the proton-to-pion peak increases with decreasing $p_{\mathrm{T}}^{\mathrm{jet}}$ and its maximum always stays at around $p_{\mathrm{T}} = 3\,\mathrm{GeV}/c$. On the contrary, in PYTHIA 8 the size of the peak does not change with $p_{\mathrm{T}}^{\mathrm{jet}}$, instead the position of the maximum is shifted to higher p_{T}.
- The multiplicity dependence of the average transverse expansion velocity is found to be more affected by jets in PYTHIA 8 than in EPOS 3.

Therefore, this analysis applied to LHC and RHIC data would allow to learn more about the origin of collectivity in pp collisions.

Acknowledgments

We acknowledge Gergely Gábor Barnaföldi, Peter Christiansen, Eleazar Cuautle, Arturo Fernández and Guy Paić for the critical reading of the manuscript and the valuable discussion and suggestions. We also acknowledge Klaus Werner for allowing us the usage of EPOS 3.117 and for the useful instructions.

Support for this work has been received from CONACYT under the grant No. 260440; from DGAPA-UNAM under PAPIIT grant IA102515. In addition, this work was supported by Hungarian OTKA grants NK106119, K120660 and NIH TET 12 CN-1-2012-0016.

References

[1] B. B. Abelev, et al., Multiplicity dependence of pion, kaon, proton and lambda production in p-Pb collisions at $\sqrt{s_{\rm NN}}$ = 5.02 TeV, Phys. Lett. **B728** (2014) 25–38. arXiv:1307.6796, doi:10.1016/j.physletb.2013.11.020.

[2] J. Adam, et al., Multiplicity dependence of charged pion, kaon, and (anti)proton production at large transverse momentum in p-Pb collisions at $\sqrt{s_{\rm NN}}$ = 5.02 TeV, Phys. Lett. **B760** (2016) 720–735. arXiv:1601.03658, doi:10.1016/j.physletb.2016.07.050.

[3] B. B. Abelev, et al., Long-range angular correlations of π, K and p in p-Pb collisions at $\sqrt{s_{\rm NN}}$ = 5.02 TeV, Phys. Lett. **B726** (2013) 164–177. arXiv:1307.3237, doi:10.1016/j.physletb.2013.08.024.

[4] V. Khachatryan, et al., Evidence for collectivity in pp collisions at the LHC, arXiv:1606.06198.

[5] J. Adam, et al., Multiplicity-dependent enhancement of strange and multi-strange hadron production in proton-proton collisions at $\sqrt{s}$ = 7 TeV, arXiv:1606.07424.

[6] J. Adam, et al., Multi-strange baryon production in p-Pb collisions at $\sqrt{s_{\rm NN}}$ = 5.02 TeV, Phys. Lett. **B758** (2016) 389–401. arXiv:1512.07227, doi:10.1016/j.physletb.2016.05.027.

[7] V. Khachatryan, et al., Multiplicity and rapidity dependence of strange hadron production in pp, ~~pPb, and PbPb~~ p-Pb, and Pb-Pb collisions at the LHC, Submitted to: Phys. Lett. BarXiv:1605.06699.

[8] R. Bala, I. Bautista, J. Bielcikova, A. Ortiz, Heavy-ion physics at the LHC: Review of Run I results, Int. J. Mod. Phys. **E25** (2016) 1642006. arXiv:1605.03939, doi:10.1142/S0218301316420064.

[9] B. B. Abelev, et al., Production of charged pions, kaons and protons at large transverse momenta in pp and Pb-Pb collisions at $\sqrt{s_{\rm NN}}$ =2.76 TeV, Phys. Lett. **B736** (2014) 196–207. arXiv:1401.1250, doi:10.1016/j.physletb.2014.07.011.

[10] J. Adam, et al., Centrality dependence of the nuclear modification factor of charged pions, kaons, and protons in Pb-Pb collisions at $\sqrt{s_{\rm NN}}$ = 2.76 TeV, Phys. Rev. **C93** (3) (2016) 034913. arXiv:1506.07287, doi:10.1103/PhysRevC.93.034913.

[11] J. Adam, et al., Measurement of charged jet production cross sections and nuclear modification in p-Pb collisions at $\sqrt{s_{\rm NN}}$ = 5.02 TeV, Phys. Lett. **B749** (2015) 68–81. arXiv:1503.00681, doi:10.1016/j.physletb.2015.07.054.

[12] A. Ortiz, Mean $p_{\rm T}$ scaling with m/n_q at the LHC: Absence of (hydro) flow in small systems?, Nucl. Phys. **A943** (2015) 9–17. arXiv:1506.00584, doi:10.1016/j.nuclphysa.2015.08.003.

[13] B. G. Zakharov, Flavor dependence of jet quenching in pp collisions and its effect on $R_{\rm AA}$ for heavy mesons, JETP Lett. 103 (6) (2016) 363–368. arXiv:1509.07020, doi:10.1134/S0021364016060126.

[14] P. Bozek, W. Broniowski, G. Torrieri, Mass hierarchy in identified particle distributions in proton-lead collisions, Phys. Rev. Lett. **111** (2013) 172303. arXiv:1307.5060, doi:10.1103/PhysRevLett.111.172303.

[15] T. Sjostrand, M. van Zijl, A Multiple Interaction Model for the Event Structure in Hadron Collisions, Phys. Rev. D36 (1987) 2019. doi:10.1103/PhysRevD.36.2019.

[16] T. Sjstrand, S. Ask, J. R. Christiansen, R. Corke, N. Desai, P. Ilten, S. Mrenna, S. Prestel, C. O. Rasmussen, P. Z. Skands, An Introduction to PYTHIA 8.2, Comput. Phys. Commun. **191** (2015) 159–177. arXiv:1410.3012, doi:10.1016/j.cpc.2015.01.024.

[17] A. Ortiz, P. Christiansen, E. Cuautle, I. Maldonado, G. Paić, Color reconnection and flowlike patterns in pp collisions, Phys. Rev. Lett. 111 (**4**). doi:10.1103/PhysRevLett.111.042001.

[18] T. Lappi, B. Schenke, S. Schlichting, R. Venugopalan, Tracing the origin of azimuthal gluon correlations in the color glass condensate, JHEP **01** (2016) 061. arXiv:1509.03499, doi:10.1007/JHEP01(2016)061.

[19] B. Schenke, S. Schlichting, P. Tribedy, R. Venugopalan, Mass ordering of spectra from fragmentation of saturated gluon states in high multiplicity proton-proton collisionsarXiv:

1607.02496.

[20] G.-L. Ma, A. Bzdak, Long-range azimuthal correlations in proton-proton and proton-nucleus collisions from the incoherent scattering of partons, Phys. Lett. **B739** (2014) 209–213. arXiv:1404.4129, doi:10.1016/j.physletb.2014.10.066.

[21] C. Bierlich, G. Gustafson, L. Lonnblad, A. Tarasov, Effects of Overlapping Strings in pp Collisions, JHEP **03** (2015) 148. arXiv:1412.6259, doi:10.1007/JHEP03(2015)148.

[22] S. Chatrchyan, et al., Study of the inclusive production of charged pions, kaons, and protons in pp collisions at $\sqrt{s} = 0.9$, 2.76, and 7 TeV, Eur. Phys. J. **C72** (2012) 2164. arXiv:1207.4724, doi:10.1140/epjc/s10052-012-2164-1.

[23] A. Ortiz, G. Bencdi, H. Bello, S. Jena, Jet effects in high-multiplicity pp events, in: Proceedings, 7th International Workshop on Multiple Partonic Interactions at the LHC (MPI@LHC 2015), 2016, pp. 215–219. arXiv:1603.05213.
URL https://inspirehep.net/record/1428679/files/arXiv:1603.05213.pdf

[24] B. Andersson, G. Gustafson, G. Ingelman, T. Sjostrand, Parton Fragmentation and String Dynamics, Phys. Rept. 97 (1983) 31–145. doi:10.1016/0370-1573(83)90080-7.

[25] X. Artru, G. Mennessier, String model and multiproduction, Nucl. Phys. B70 (1974) 93–115. doi:10.1016/0550-3213(74)90360-5.

[26] K. Werner, B. Guiot, I. Karpenko, T. Pierog, Analysing radial flow features in p-Pb and p-p collisions at several TeV by studying identified particle production in EPOS3, Phys. Rev. **C89** (6) (2014) 064903. arXiv:1312.1233, doi:10.1103/PhysRevC.89.064903.

[27] K. Werner, I. Karpenko, T. Pierog, M. Bleicher, K. Mikhailov, Evidence for hydrodynamic evolution in proton-proton scattering at 900 GeV, Phys. Rev. **C83** (2011) 044915. arXiv:1010.0400, doi:10.1103/PhysRevC.83.044915.

[28] T. Martin, P. Skands, S. Farrington, Probing Collective Effects in Hadronisation with the Extremes of the Underlying Event, Eur. Phys. J. **C76** (5) (2016) 299. arXiv:1603.05298, doi:10.1140/epjc/s10052-016-4135-4.

[29] S. Porteboeuf, T. Pierog, K. Werner, Producing Hard Processes Regarding the Complete Event: The EPOS Event Generator, in: Proceedings, 45th Rencontres de Moriond on Electroweak Interactions and Unified Theories, 2010. arXiv:1006.2967.
URL https://inspirehep.net/record/858343/files/arXiv:1006.2967.pdf

[30] P. Skands, S. Carrazza, J. Rojo, Tuning PYTHIA 8.1: the Monash 2013 Tune, Eur. Phys. J. **C74** (8) (2014) 3024. arXiv:1404.5630, doi:10.1140/epjc/s10052-014-3024-y.

[31] M. Cacciari, G. P. Salam, G. Soyez, FastJet User Manual, Eur. Phys. J. **C72** (2012) 1896. arXiv:1111.6097, doi:10.1140/epjc/s10052-012-1896-2.

[32] J. Adam, et al., Measurement of jet suppression in central Pb-Pb collisions at $\sqrt{s_{\rm NN}} = 2.76$ TeV, Phys. Lett. **B746** (2015) 1–14. arXiv:1502.01689, doi:10.1016/j.physletb.2015.04.039.

[33] X. Lu, Measurement of hadron composition in charged jets from pp collisions with the ALICE experiment, Nucl. Phys. **A931** (2014) 428–432. arXiv:1407.8385, doi:10.1016/j.nuclphysa.2014.08.003.

[34] M. Veldhoen, p/π Ratio in Di-Hadron Correlations, Nucl. Phys. **A910-911** (2013) 306–309. arXiv:1207.7195, doi:10.1016/j.nuclphysa.2012.12.103.

[35] X. Zhang, $\rm K^0_S$ and Λ production in charged particle jets in p-Pb collisions at $\sqrt{s_{\rm NN}} = 5.02$ TeV with ALICE, Nucl. Phys. **A931** (2014) 444–448. arXiv:1408.2672, doi:10.1016/j.nuclphysa.2014.08.102.

[36] E. Schnedermann, J. Sollfrank, U. W. Heinz, Thermal phenomenology of hadrons from 200-A/GeV S+S collisions, Phys. Rev. **C48** (1993) 2462–2475. arXiv:nucl-th/9307020, doi:10.1103/PhysRevC.48.2462.

[37] A. Ortiz, G. Paić, E. Cuautle, Mid-rapidity charged hadron transverse spherocity in pp collisions simulated with Pythia, Nucl. Phys. **A941** (2015) 78–86. arXiv:1503.03129, doi:10.1016/j.nuclphysa.2015.05.010.